Journal of Electroanalytical Chemistry xxx (xxxx) 117312

Contents lists available at ScienceDirect

Journal of Electroanalytical Chemistry

journal homepage: www.elsevier.com/locate/jelechem

Electrochemical immunoplatform to help managing pancreatic cancer

Víctor Pérez-Ginés [a], Rebeca M. Torrente-Rodríguez [a], María Pedrero [a], Neus Martínez-Bosch [b], Pablo García de Frutos [c], Pilar Navarro [b, d, *], José M. Pingarrón [a, *], Susana Campuzano [a, *]

[a] Departamento de Química Analítica, Facultad de CC. Químicas, Universidad Complutense de Madrid, 28040 Madrid, Spain
[b] Cancer Research Program, Hospital del Mar Medical Research Institute (IMIM), Unidad Asociada IIBB-CSIC, Barcelona, Spain
[c] Department of Cell Death and Proliferation, IIBB-CSIC, Unidad Asociada IMIM/IIBB-CSIC, Centro de Investigación Biomédica en Red de Enfermedades Cardiovasculares (CIBERCV), and Institut d'Investigacions Biomèdiques August Pi Sunyer (IDIBAPS), Barcelona, Spain
[d] Department of Cell Death and Proliferation, Institute of Biomedical Research of Barcelona (IIBB)-CSIC and Institut d'Investigacions Biomèdiques August Pi Sunyer (IDIBAPS), Barcelona, Spain

ARTICLE INFO

Keywords:
Immunoplatform
Amperometry
CA19-9
Pancreatic cancer
Serum samples

ABSTRACT

Pancreatic ductal adenocarcinoma (PDAC) is the solid tumor with the worst prognosis, representing today the third cause of cancer-related deaths in developed countries and expected to be the second in 2030. Today, CA19.9 remains the only clinically used marker for management of PDAC (FDA-approved as a disease monitoring marker). This work reports a disposable amperometric immunoplatform for the determination of CA19-9. The immunoplatform skilfully combines the advantages of magnetic microsupports (MBs) for implementation of the immunoassay and amperometric transduction on screen-printed carbon electrodes (SPCEs). The method involves the preparation of sandwich immunocomplexes enzymatically labeled with the enzyme horseradish peroxidase (HRP) on the MBs and uses a detection antibody conjugated to HRP. Once the HRP-labeled sandwich immunocomplexes-bearing MBs were trapped on the SPCE surface, the variation of the cathodic current was measured in the presence of H_2O_2 and hydroquinone (HQ). This current, which was directly proportional to the concentration of CA19-9. Under the optimized experimental conditions, the immunoplatform allowed the amperometric determination of CA19-9 standards over the 5 to 500 U mL^{-1} concentration range, with a limit of detection (LOD) value of 1.5 U mL^{-1} in 1 h. The method exhibits good reproducibility and selectivity and the magnetic immunoconjugates shows a good storage stability. The immunoplatform was applied to the determination of CA19-9 in serum samples of a medium-sized cohort (22 individuals) of healthy subjects and patients diagnosed with PDAC. The obtained results demonstrated the immunoplatform ability to discriminate both types of individuals within 1 h after sample dilution. The developed immunoplatform represents an improvement in terms of cost, applicability and accessibility compared to the ELISA-based techniques currently used in the clinic.

1. Introduction

Among all plausible manifestations of human cancer, epidemiological studies describe that pancreatic ductal adenocarcinoma (PDAC), the main subtype of pancreatic cancer [1], ranks as the most lethal neoplasm with five-year overall survival rates of 11 % [2–5]. To improve this dismal prognosis, detection of PDAC at the earliest stages is greatly demanded. However, the lack of well-validated and specific screening tests and the compromised positive predictive value of the diagnostic procedures available, which may lead to over-diagnosis and overtreatment, remain the two main problems to overcome [6,7].

In terms of a screening standpoint, clinical markers with biologically distinct omic origin, including proteins, microRNAs, exosomes, circulating and methylated DNA, antibodies, and metabolites have been tested in multiplexed panels for PDAC screening [8]. All of them except one, the carbohydrate antigen 19–9 (CA19-9), showed an important lack of applicability in longitudinal screening, thus demonstrating that they are not yet mature enough for translation to clinical practice. Accordingly, CA19-9 is the unique tumor biomarker accepted by the US Food and Drug Administration for PDAC diagnosis and treatment monitoring [9–12].

Traditionally, imaging-based methods have been used for the diagnostic finding of early-stage PDAC. These methods include computed

* Corresponding authors at: Cancer Research Program, Hospital del Mar Medical Research Institute (IMIM), Unidad Asociada IIBB-CSIC, Barcelona, Spain (P. Navarro).
E-mail addresses: pilar.navarro@iibb.csic.es (P. Navarro), pingarro@quim.ucm.es (J.M. Pingarrón), susanacr@quim.ucm.es (S. Campuzano).

https://doi.org/10.1016/j.jelechem.2023.117312
Received 29 January 2023; Received in revised form 20 February 2023; Accepted 7 March 2023
1572-6657/

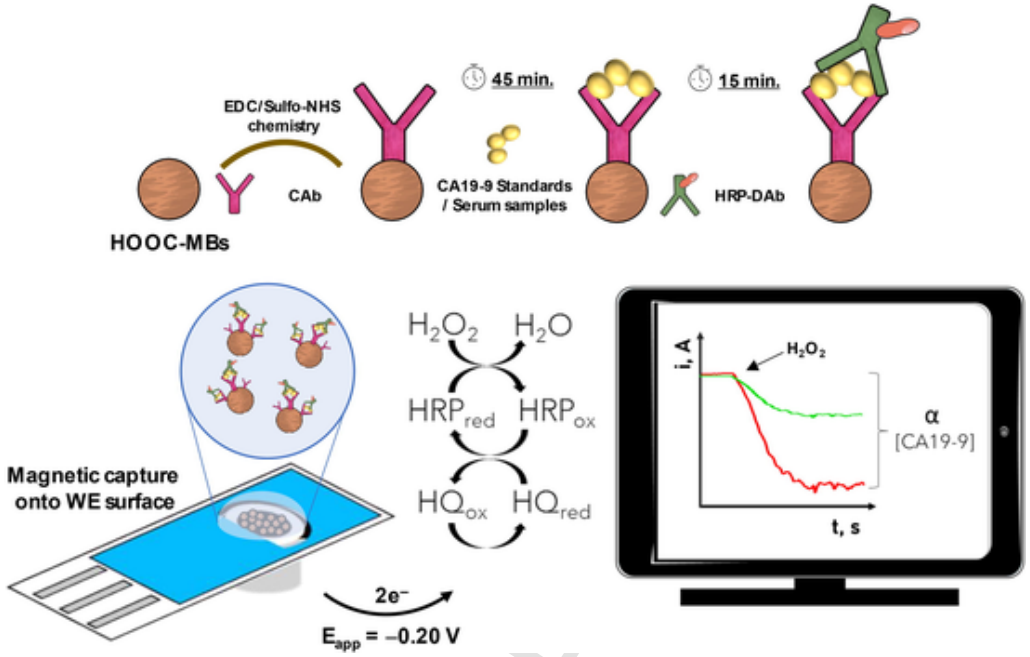

Scheme 1. Schematic diagram of the protocol used for the formation of sandwich-type immunocomplexes on magnetic microcarriers, and the enzymatic and electrochemical reactions involved in the amperometric transduction on SPCEs.

tomodensitometry (CT), endoscopic ultrasound (EUS), abdominal ultrasound and magnetic resonance imaging (MRI) [13]. Nevertheless, significant diagnostic challenges related to these methods persist, mainly due to difficulties in localizing small PDAC lesions (as they may be partially masked by gas interference in the gastrointestinal tract), decreased diagnostic sensitivity when PDAC tumors are smaller than 2 cm, poor specificity, and subjectivity of clinicians for early detection [14]. Other methodologies currently used to diagnose PDAC comprise a combination of radiological proofs with typical clinical evidence, followed by diagnostic confirmation of the pathologic state by fine needle aspiration or brush cytology. These methods have the limitations of being invasive and time-consuming [15]. However, invasive tissue biopsies of primary or metastatic lesions remain the gold standard for PDAC diagnosis, although repeat sampling is infeasible. This is why noninvasive liquid biopsies offer new opportunities for early diagnosis in high-risk cohorts and for longitudinal analysis of tumor evolution and progression in patients undergoing treatment [16]. Thus, the exploration of tumor biomarkers detectable in blood has an essential utility not only to accurately identify patients in the early stages of tumor growth, but also to estimate response to treatment or recurrence [17–20].

CA19-9, also known as Sialyl Lewis A (sLeA) antigen, is the most widely used non-invasive blood-based diagnostic tumor biomarker to confirm suspected PDAC [21], as it is highly expressed and released by cancerous pancreatic cells [22,23]. CA19-9 is created by deregulated glycosylation, which occurs aberrantly during cancer progression resulting in the formation of multiple glycosylated residues. Considering that this type of modification is regarded as one of the cancer hallmarks, this antigen emerged as a potential PDAC-related proteomic entity for a long time [24] and has remained useful to the present day. Serum CA19-9 levels below 37 U mL^{-1} are considered normal [25].

It is well-accepted that multiplexed biomarker assays allow more accurate and precise cancer diagnostics and prognosis compared to single biomarker assays. This is especially true for discrimination of pathologies that are hardly distinguishable in a clinical setting, like PDAC and chronic pancreatitis, a non-cancerous inflammation of the organ. However, multiplex biomarker requires additional optimization and has higher costs, therefore it is not currently used for population screening, nor diagnosis/prognosis of PDAC. In contrast, CA19-9, despite some limitations like false negatives in people not expressing the Lewis antigen due to FUT3 mutations and false positives in non-malignant pancreatic inflammatory disease, has still reasonable accuracy (79 % sensitivity and 82 % specificity) to be used as single biomarker for PDAC. It stands out especially for patient follow-up to monitor therapy response and/or predict tumor relapse. Furthermore, although serum CA19-9 levels are also increased in various cancer types and subtypes, including colorectal cancer (CRC), gastric cancer, ovarian cancer, and bile duct cancer, it has been shown that the highest sensitivity and selectivity is achieved in patients with PDAC [26–28]. Furthermore, single CA19-9 analysis is apt enough to yield valuable information related to PDAC aggressiveness in differentially pooled subsets, including patients with stage I-II and those stratified into stage III-IV [29].

Accordingly, given the usefulness of CA19-9 to assess the presence and progression of PDAC, the development of rapid and accurate methods for the easy, affordable, and sensitive monitoring of this biomarker remains a compelling goal for the scientific and clinical communities. In this context, in the last decade, the unique advantages exhibited by electrochemical biosensors in terms of simplicity, affordability and point-of-care (POC) applicability have been exploited to develop methods for the determination of CA19-9 [30–44]. However, most of these biosensors require the use of nanomaterials and long fabrication times and none of them have been implemented taking advantage of the benefits inherent to the use of micromagnetic supports in terms of improved sensitivity, fast kinetics, and minimization of matrix effect [45,46].

This work reports a simple, but highly competitive electrochemical (EC) immunoplatform compared to other more complex methodologies displayed up to date for the determination of CA19-9. Notable are its achievements in terms of rapidity of analysis, affordability, and POC capabilities in serological samples collected from PDAC patients and control individuals. The developed EC-immunosystem relies on a sandwich-type configuration using an antibody pair consisting of selective capture and HRP-conjugated detector immunoglobulins. The formed immunocomplex stays conveniently immobilized onto the surface of previously activated magnetic micro-supports (MBs) containing functional surface carboxylic groups. The modified MBs are captured on

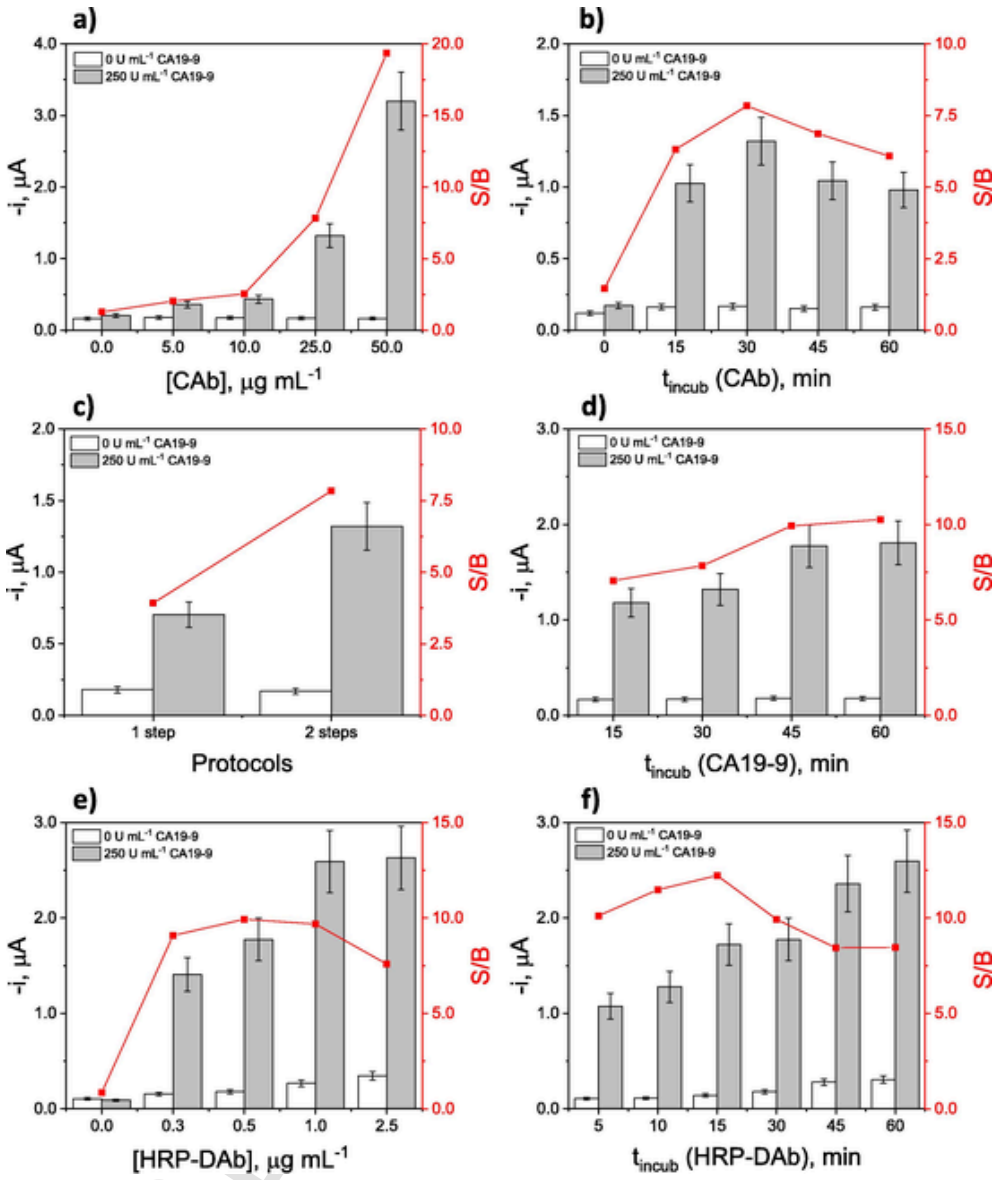

Fig. 1. Optimization of key experimental variables involved in the formation of sandwich immunocomplexes on MBs. Comparison of the amperometric responses for 0 (signal B) and 250 (signal S) U mL^{-1} of CA19-9 standard provided by bioplatforms prepared using magnetic bioconjugates involving CAb-MBs by varying: a) CAb concentration and b) incubation time, c) number of steps involved in the formation of immunocomplex, d) incubation time of CAb-MBs with CA19-9 solution, e) concentration and f) incubation time with HRP-DAb solution.

screen-printed carbon electrodes (SPCEs) to perform amperometric transduction in the presence of H_2O_2 and hydroquinone (HQ).

2. Experimental section

2.1. Apparatus and electrodes

A CHI1140A potentiostat (CH Instruments) operated by the CHI1140A software was employed for the electrochemical measurements. Screen-printed carbon electrodes (SPCEs, DRP-110) and their connecting cable (DRP-CAC) were purchased from Metrohm Hispania. Magnetic trapping of modified microbeads (MBs) on the working electrode (WE) surface was controlled by a neodymium magnet (AIMAN GZ) embedded in a homemade polymethylmethacrylate (PMMA) casing. A magnetic particle concentrator (DynaMag™-2, Invitrogen) was used to separate and handle MBs. ELISA tests were performed with a SPECTROstar Nano ELISA plate reader (BMG Labtech), a Digital rocking SHAKER S-4 (ELMI) and flat-bottom ELISA plates.

Other used instruments were a BioSan TS-100 uniform temperature incubator shaker (Thermo), a vortex (Velp Scientifica), a magnetic stirrer (Inbea), and a Basic pH-meter (Basic 20 + , Crison).

2.2. Reagents and solutions

Magnetic microbeads functionalized with carboxylic acid groups (HOOC-MBs, M−270) and 1-(3-dimethylaminopropyl)-3-ethylcarbodiimide hydrochloride (EDC) were purchased from Thermo Fisher Scientific, *N*-hydroxysulfosuccinimide (sulfo-NHS) from Fluorochem, and 2-(*N*-morpholino)ethanesulfonic acid (MES) and bovine serum albumin (BSA) were from Gerbu. Human CA19-9 standard, mouse anti-human CA19-9 (used as capture antibody, CAb), and HRP labeled mouse anti-human CA19-9 (used as detector antibody, HRP-DAb) were acquired from Genetex (refs. GTX02886-pro, GTX635389 and GTX635391, respectively). Sodium chloride (NaCl), tris(hydroxymethyl)aminomethane (Tris), potassium chloride (KCl), dihydrated sodium di-hydrogen phosphate ($NaH_2PO_4{\cdot}2H_2O$) and anhydrous di-

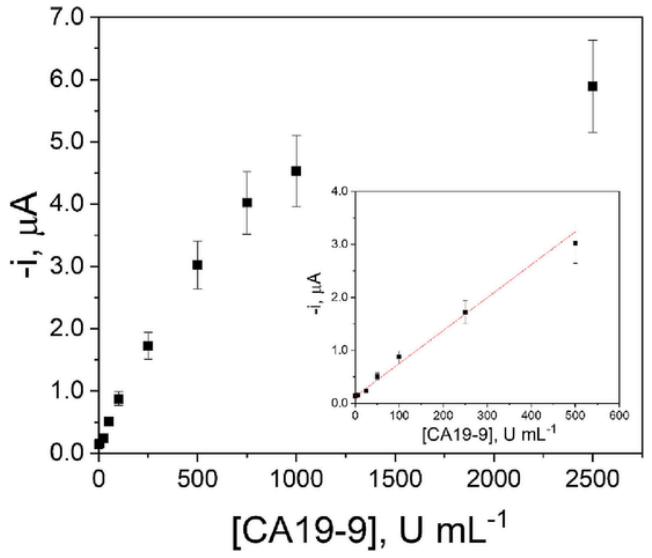

Fig. 2. Dependence of the cathodic current variations provided by the developed amperometric immunoplatform with the concentration of CA19-9 standards. Inset: obtained linear dependence.

sodium hydrogen phosphate (Na_2HPO_4) were obtained from Scharlab. Blocker casein (BB, phosphate-buffered saline (PBS) containing 1.0 % w/v casein, pH 7.4) and 3,3́,5,5-tetramethylbenzidine (TMB) commercial solutions were ordered from Thermo Fisher Scientific, and sodium hydroxide (NaOH) from Labkem. Hydroquinone (HQ), hydrogen peroxide (H_2O_2) (30 %, w/v), ethanolamine and Tween® 20 from Sigma-Aldrich and Stop Solution (2 N H_2SO_4) from Cayman Chemicals were also used.

The following human protein standards were evaluated as potential interfering compounds: hemoglobin (Hb, ref. H7379) and human immunoglobulin G (hIgG, ref. I2511) from Sigma-Aldrich, growth arrest-specific 6 (GAS6, ref. DY885B), interleukin 1 receptor-like 1 (IL1RL1/IL33R/ST2, ref. DY523B-05), cluster of differentiation 147 (CD147, ref. DY972), E-cadherin (E-Cad, ref. DYC4225), interleukin-13 receptor alpha2 (IL-13Rα2, ref. DY614) and hypoxia inducible factor 1 alpha (HIF-1α, ref. DYC1935) from R&D Systems, human serum albumin (HSA, Sigma Life Science, ref. A1653), cadherin-17 (CDH-17, OriGene Technologies, ref. TP720740), and tumor necrosis factor alpha (TNF-α, BD Pharmigen, ref. 55,618). All the employed reagents were of the highest available grade.

Used buffer solutions, prepared with deionized water from a Millipore Milli-Q purification system (18.2 MΩ·cm) include: 0.025 M MES, pH 5.0; phosphate-buffered saline (PBS) which consists of 0.01 M phosphate buffer solution with 137 mM NaCl and 2.7 mM KCl, pH 7.4; 0.1 M phosphate buffer (PB), pH 8.0; 0.1 M Tris-HCl, pH 7.2; and 0.05 M PB, pH 6.0. Wash buffer (0.05 % Tween® 20 in PBS), blocking buffer (2.5 % BSA in PBS) and reagent diluent (1 % BSA in PBS) were used for the ELISA method. For electrochemical measurements, 0.1 M HQ and H_2O_2 solutions, were prepared daily in 0.05 M PB (pH 6.0) just before use.

2.3. Formation of HRP enzymatically labeled sandwich immunocomplexes on magnetic microsupports and amperometric detection

Sequential biofunctionalization of the HOOC-MBs was performed under continuous stirring (950 rpm) at 25 °C in 1.5 mL microcentrifuge tubes. After each modification step, MBs were washed twice with 50 μL of the corresponding buffer and magnetized for 3 min using a concentrator before removing the supernatant. Firstly, a 3 μL-aliquot of the commercial HOOC-MBs suspension (homogenized by vortexing) was placed in the centrifuge tube and, after two washing steps with MES buffer for 10 min, the surface carboxylic groups were activated with 25 μL of a mixture solution containing EDC and sulfo-NHS 50 mg mL^{-1} each in MES buffer for 35 min. Activated MBs were washed twice with MES and incubated for 30 min with 25 μL of a 25 μg mL^{-1} CAb solution prepared in MES. After a further washing with MES, the redundant active sites in the EDC/sulfo-NHS activated MBs were sealed by incubation with 25 μL of a 1.0 M ethanolamine solution (prepared in PB, pH 8.0) for 60 min. The CAb-MBs were then washed once with Tris-HCl buffer, twice with PBS, and stored at 4 °C in filtered PBS until required for the target determination. Sandwich immunocomplexes were formed by two successive incubation steps with 25 μL of a solution containing the CA19-9 standard (or the analyzed sample) in PBS for 45 min, and 25 μL of 0.5 μg mL^{-1} HRP-DAb in BB for 15 min, mediating two washings with BB between these steps. The resulting magnetic bioconjugates were subsequently washed with BB and then resuspended in 50 μL of PB, pH 6.0.

After placing a SPCE in the PMMA casing, a 50 μL aliquot of resuspended MBs in PB was pipetted and magnetically captured onto the WE surface. The SPCE/magnetic housing assembly was connected to the potentiostat and immersed into an electrochemical cell containing 10 mL of PB, pH 6.0, supplemented with freshly prepared 1.0 mM HQ under continuous stirring. Amperometric measurements were performed at –0.20 V (*vs.* the Ag pseudo-reference electrode) upon addition of 50 μL of a freshly prepared 0.1 M H_2O_2 solution once the background current was stabilized. The provided signals given in the manuscript were calculated as the difference between the steady-state and background currents. Given error bars were estimated as three times the standard deviation of three replicates (confidence intervals calculated for $\alpha = 0.05$).

2.4. Analysis of serum samples from healthy individuals and pancreatic cancer patients.

The developed immunosensor was applied to the determination of CA19-9 in serum samples from control individuals and from patients diagnosed with PDAC provided by the Hospital del Mar Medical Research Institute (IMIM), after approval of the corresponding Ethic Committee (IMIM 2020/9067/I) and was implemented in accordance with the Helsinki Declaration of Principles. All individual participants voluntarily signed an informed consent allowing the use of their serum samples for research purposes.

Once the absence of matrix effect was confirmed, quantification was performed by simple interpolation of the amperometric responses provided by the immunosensor for 50-fold diluted serum samples into the calibration graph constructed with CA19-9 standards. The serum samples were also analyzed as well as by ELISA using the same immunoreagents. The ELISA methodology is similar to that reported by Muñoz-San Martín et al. [47], working with solutions of 5 μg mL^{-1} CAb, 100 ng mL^{-1} HRP-DAb and 100-times diluted serum samples as well as interpolation into the calibration graph constructed with CA19-9 standards over the 50 to 250 U mL^{-1} concentration range. Moreover, to compare these CA19-9 values obtained from the immunosensor or ELISA with those from the clinic diagnostics, the same samples were also tested at the Laboratori de Referència de Catalunya (Barcelona, Spain) using an electrochemiluminescent technique (ECLIA), which involves the use of the monoclonal antibody 1116-NS-19–9 and a Cobas 4000 analyzer (Roche Diagnostics).

3. Results and discussion

The rationale of the proposed immuno-strategy for the determination of the carbohydrate antigen CA19-9 (Scheme 1) relied on the exploitation of carboxyl-functionalized magnetic microsupports (HOOC-MBs) on which specific anti-CA19-9 (CAb) antibodies, able to efficiently and specifically recognize the target antigen, were covalently

Table 1
Comparison of the analytical/operational features and applications of electrochemical immunosensors/immunoassays reported for the determination of CA19-9 in the last decade.

Rationale	Technique	LR	LOD	Preparation/ Determination time	Storage stability / other remarkable features	Applicability	Ref.
Reagentless label-free direct immunosensor at a GCE modified with Fe_3O_4@SiO_2–Au@mSiO_2, MWCNTs and GOD	DPV (glucose) "Signal off"	0.01–1.11 and 11.11–476.11 U mL^{-1}	0.004 U mL^{-1}	~26 h/~ 45 min	25 days / Reagentless, DET	–	[29]
Sandwich type immunosensor using a AuNPs-AuE and Nafion-coated TiO_2 composite nanoparticles (NTs) decorated with DAb + $Co(dcbpy)_3^{2+}$ or DAb + MB for dual determination of CA19-9 and CA15.3	DPV ($Co(dcbpy)_3^{2+}$) "Signal on"	5–100 U mL^{-1}	1.6 U mL^{-1}	8.5 h (DAb + $Co(dcbpy)_3^{2+}$/ NTs: 8.5 h)/2h	–	Spiked serum samples	[30]
Sandwich-type electrochemical immunosensor based on b-cAb immobilization on a SA-3DOMM (Au–Fe_3O_4@SiO_2) AuE, HRP-DAb/Au@SBA-15	Chronoamperometry (H_2O_2) "Signal on"	0.05–15.65 U mL^{-1}	0.01 U mL^{-1}	b-CAb-SA-3DOMM: 15 h (Au–Fe_3O_4@SiO_2: 6.5 h; HRP-DAb/Au@SBA-15: 20 h 20 min)/2h	30 days/ Regeneration: ≥ 5 cycles, DET	Serum samples	[31]
Label-free direct immunosensor at a PThi-SDS/AuNPs-GCE	DPV (PThi) "Signal off"	5–400 U mL^{-1}	0.45 U mL^{-1}	1 h (PThi-SDS: 36 h)/1h	20 days: 88.6% initial current	–	[32]
Electrochemical microfluidic chip for multiplex determination of CEA, CA19-9, H.P., P53, PG I and PG-II involving Label-free direct immunosensing formats CAb covalently immobilized onto Au microelectrodes modified with mercaptoacetic acid and EDC/ NHS	DPV ($[Fe(CN)_6]^{4-/3-}$) "Signal-off"	10.75–172 U mL^{-1}	10.75 U mL^{-1}	5 h 20 min/35 min	–	Serum specimens of gastric cancer patients	[33]
Label-free direct immunosensor at a AuNPs@PThi-GCE	DPV (PThi) "Signal off"	6.5–520 U mL^{-1}	0.26 U mL^{-1}	13 h (AuNPs@PThi: 24 h)/1h	–	Serum samples from PDAC patients	[34]
Label-free direct immunosensor developed at a GCE modified with AuPt NCs	DPV ($[Fe(CN)_6]^{4-/3-}$) "Signal-off"	0.05–50 U mL^{-1}	0.03 U mL^{-1}	~ 2 h / --	7 days / --	Spiked human serum samples	[35]
Label-free direct immunosensor developed by NHS-assisted covalent immobilization of CAb on interdigitated AuEs combining PEI and MWCNTs	EIS (capacitance)	–	0.35 U mL^{-1}	1 h 25 min/10 min	–	Cell lysates and blood serum	[36]
Label-free direct immunosensor developed at a interdigitated AuEs modified with a 11-MUA SAM activated with NHS and EDC and a layer of anti-CA19-9 antibodies	EIS ($[Fe(CN)_6]^{4-/3-}$) "Signal-on"	4–189 U mL^{-1}	0.68 U mL^{-1}	10 h / 10 min	–	Two cell lines supernatant samples, HT-29 (12.26 U mL^{-1} of CA19-9) and SW-620 (no detectable levels of CA19-9) . Serum samples from 8 PDAC patients.	[37]
Label-free direct immunosensor developed by adsorbing CAb at SPIDE/CNO-GO	EIS (capacitance)	0.3–100 U mL^{-1}	0.12 U mL^{-1}	SPIDE/CNO-GO: 5 h (GO: 14 h)/10 min	–	Commercial samples and cell lines lysates tested positive (HT29) and negative (SW620) for CA19-9	[38]
Label-free direct immunosensor developed by adsorbing CAb at SPCEs coated LbL films of CB and polyelectrolytes (PEI and PAA)	DPV ($[Fe(CN)_6]^{4-/3-}$) "Signal-off"	0.01–40 U mL^{-1}	0.07 U mL^{-1}	~ 15 h / 20 min	2 weeks	Cell lysates of CRC from HT-29 and SW-620 cell lines and serum from cancer patients	[39]

(*continued on next page*)

Table 1 (*continued*)

Rationale	Technique	LR	LOD	Preparation/ Determination time	Storage stability / other remarkable features	Applicability	Ref.
Label-free direct immunosensor developed at a GCE modified with a CS-MWCNT-Fe_3O_4 nanocomposite	SWV ($[Fe(CN)_6]^{3-/4-}$)	1.0 pg mL^{-1} – 100 ng mL^{-1}	0.163 pg mL^{-1}	3 h 30 min (CS-MWCNT-Fe_3O_4: 15 h) / 30 min	15 days	Serum samples from endometriosis patients	[40]
Label-free direct immunosensor developed at a GCE modified with rGO and 3D biomimetic hydrangea-like bismuth oxychloride (BiOCl) and PtNi nanocubes	DPV ($[Fe(CN)_6]^{4-/3-}$] "Signal-off"	0.01–150 U mL^{-1}	0.0034 U mL^{-1}	~ 14 h (~15 h rGO, ~ 28 h BiOCl-APTES-PtNi composite) / 2 h	9 days	Clinical patient blood samples	[41]
Label-free direct immunosensor developed at a GCE modified with Fe_3O_4@NPCS	DPV ($[Fe(CN)_6]^{4-/3-}$] "Signal-off"	0.00001–10 U mL^{-1}	2.49 × 10^{-6} U mL^{-1}	13.5 h (Fe_3O_4@NPCS: 34 h)/1h	4 weeks	Spiked serum samples	[42]
Sandwich immunosensor involving a GS/Thi-GCE and MXene/HRP/DAb	DPV (Thi/H_2O_2) "Signal-on"	0.002–30 U mL^{-1}	0.001 U mL^{-1}	≥ 0.5 h (MXene/HRP/DAb: 1 h)/ ≥ 2 h	–	Serum samples	[43]
Label-free direct immunosensor prepared by covalent immobilization of the CAb using EDC/NHS on a AuE modified with a binary SAM of MPA and MCH	DPV ($[Fe(CN)_6]^{4-/3-}$] "Signal-off"	0.05–500 U mL^{-1}	0.01 U mL^{-1}	~37 h/0.5 h	3 weeks: 85% initial sensitivity	Spiked serum samples	[44]
HRP-labeled sandwich immunoassay implemented on the surface of HOOC-MBs and electrochemical transduction at SPCEs	Amperometry (H_2O_2/HQ)	5–500 U mL^{-1}	1.5 U mL^{-1}	2 h 5 min/1h	CAb-MBs: 21 days	Serum samples from healthy and PDAC patients	This work

APTES: 3-aminopropyl)triethoxysilane; AuPt NCs: AuPt nanocalliandras; CA19-9: carbohydrate antigen 19–9; CB: carbon black; CEA: carcinoembryonic antigen; CNOs: carbon nano-onions; CS: chitosan; DAb: detector antibody; DET: direct electron transfer; DPV: differential pulse voltammetry; EDC: 1-ethyl-3-[3-dimethylaminopropyl] carbodiimide hydrochloride; EIS: electrochemical impedance spectroscopy; 3DOMM: three dimensional ordered macroporous magnetic; GO: graphene oxide; GS: graphene sheet; H.P.: Helicobacter pylori CagA protein; HQ: hydroquinone; LbL: layer-by-layer; LOD: limit of detection; L.R.: linear range; MCH: mercaptoethanol; MPA: 3-mercaptopropionic acid; 11-MUA: 11-mercaptoundecanoic acid; NHS: *N*-hydroxysuccinimide; P53: P53 oncoprotein; PDAC: pancreatic ductal adenocarcinoma; PEI: polyethyleneimine; PG I: pepsinogen I; PG-II: pepsinogen II; PThi: polythionine; rGO: reduced graphene oxide; SPCEs: screen-printed carbon electrodes; SPIDEs: screen-printed interdigitated electrodes; SWV: square wave voltammetry.

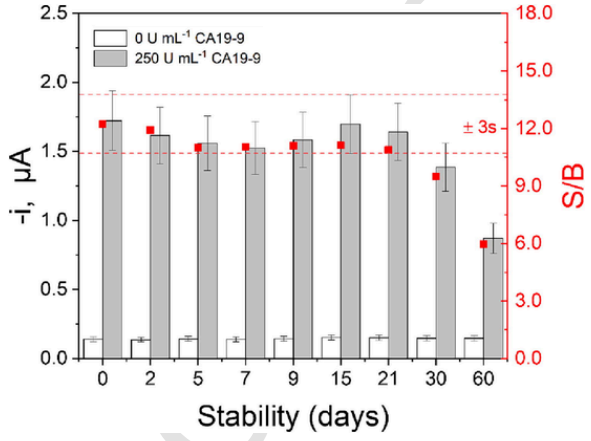

Fig. 3. Storage stability of CAb-MBs. S/B ratio values provided by bioplatforms prepared from stored CAb-MBs (in filtered PBS at 4 °C) for 0 and 250 U mL^{-1} CA19-9 standards. Control limits were set at ± 3 s of the mean value provided by 3 immunoplatforms prepared on the day of CAb-MBs manufacture.

immobilized by using carbodiimide and succinimide as chemical linkers. The selectively captured target CA19-9 was sandwiched with an HRP-labeled anti-CA19-9 detector antibody (HRP-DAb), and the resulting magnetic bioconjugates were captured on the working electrode surface of a SPCE. Amperometric transduction (E_{app} = – 0.20 V *vs.* Ag pseudo-reference electrode) was performed in stirred solutions employing hydroquinone and H_2O_2 as mediator and enzyme substrate, respectively. According to the immunoassay format, as well as the sequence of the enzymatic and electrochemical reactions involved in the transduction mechanism displayed in the scheme, the variation of the measured cathodic current was directly proportional to the CA19-9 concentration.

3.1. Optimization of key experimental variables

The determinant working variables for the formation of the HRP-labeled sandwich immunocomplexes on the surface of the magnetic microcarriers were optimized. Univariate studies were performed by comparing the amperometric responses obtained in the absence and in the presence of a fixed concentration of CA19-9 standard (blank, B, and signal, S, respectively), through the change of the variable under evaluation in a given interval, leaving the rest fixed. In general, the value of the corresponding specific variable for which a better discrimination (larger S/B ratio) and reproducibility were obtained was selected for further work.

The evaluated experimental variables were the concentration of the capture and detection antibodies (CAb and HRP-DAb, respectively), the incubation times of all immunoreagents (CAb, CA19-9 antigen, and HRP-DAb), and the number of steps used to form the sandwich-type immunocomplexes on the MBs. Other used experimental variables, such as the amount of HOOC-MB employed per determination and all the variables involved in the amperometric transduction were previously optimized [48–51].

Fig. 1 shows the dependencies of the S and B amperometric responses and the S/B ratio for the determination of CA19-9 standards when each of the studied variables was independently modified.

As Fig. 1a shows, the S/B ratio increased with the CAb concentration reaching the largest ratio at the highest tested concentration. How-

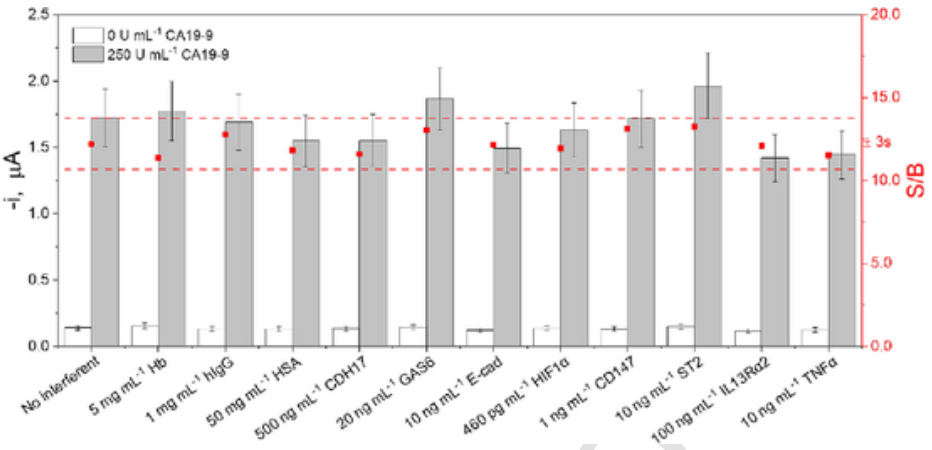

Fig. 4. Evaluation of the effect of potential interferents on the amperometric responses provided by the developed immunoplatform for 0 and 250 U mL^{-1} CA19-9 standards prepared in the absence and presence of different serum components at the indicated concentrations corresponding to the levels found in samples of healthy individuals. White bars correspond to the amperometric responses provided by the bioplatform for solutions containing only the evaluated interferent while the grey bars show results for solutions containing the interferent and CA19-9.

Table 2
Endogenous CA19-9 concentrations determined using the developed immunoplatform in serum samples of healthy individuals and patients diagnosed with PDAC. The results are compared with those provided by the ELISA methodology using the same immunoreagents, and by the ECLIA method from Barcelona's Reference Laboratory.

		Immunoplatform		ELISA		ECLIA
		[CA19-9], U mL^{-1*}	$RSD_{n=3}$, %	[CA19-9], U mL^{-1*}	$RSD_{n=3}$, %	[CA19-9], U mL^{-1}
Healthy controls	1	ND	-	ND	-	9.0
	2	ND	–	ND	–	20.4
	3	ND	–	150 ± 20	6.3	4.8
	4	130 ± 20	10.2	170 ± 30	10.9	31.9
	5	ND	–	ND	–	5.5
	6	ND	–	ND	–	0.8
PDAC patients	1	720 ± 90	6.4	790 ± 60	4.4	807.7
	2	ND	–	ND	–	26.3
	3	1300 ± 200	7.4	1200 ± 200	9.5	913.7
	4	1400 ± 100	5.4	1400 ± 100	3.7	307.1
	5	3500 ± 500	7.2	3200 ± 600	9.6	200.4
	6	18000 ± 1000	3.9	20000 ± 2000	4.5	11721.0
	7	ND	–	ND	–	251.0
	8	ND	–	ND	–	109.1
	9	270 ± 20	4.0	260 ± 20	5.0	323.4
	10	4800 ± 800	9.1	4200 ± 600	7.4	6.9
	11	1200 ± 200	9.6	1300 ± 100	5.8	1535.0
	12	9000 ± 1000	8.1	10000 ± 1000	7.6	3491.0
	13	31000 ± 4000	6.8	33000 ± 6000	9.5	19060.0
	14	43000 ± 6000	7.3	42000 ± 7000	8.9	46080.0
	15	17000 ± 2000	6.1	15000 ± 2000	7.4	747.6
	16	190 ± 10	3.3	130 ± 20	6.5	141.1

*mean value ± $ts/\sqrt{n}$; n = 3; α = 0.05. ND: Non-detectable (< LOD of 1.5 U mL^{-1}).

ever, as the signals measured working with 25 µg mL^{-1} CAb was sufficient to determine CA19-9 at clinically relevant concentrations (see below), we selected this concentration to not unnecessarily increase the cost per determination. Obviously, if a particular application required greater sensitivity this would be achieved simply by incubating the activated MBs with a larger CAb concentration (note that the S/B ratio increased from 7.8 to 19.4 when the CAb concentration changed from 25 to 50 µg mL^{-1}). Fig. 1b shows a larger S/B ratio resulted when activated MBs were incubated in CAb solution for 30 min. The slight decrease observed for longer incubation times was attributed to the smaller S responses. These were most likely due to hindered antigen recognition when many CAb molecules were immobilized on the MBs, which caused crowding or overlapping of antigen binding fragments of antibodies [52].

The results obtained using two different protocols for the preparation of the sandwich-type immunocomplexes on the CAb-MBs were compared. The protocols involved the capture of the antigen and its recognition by the detection antibody jointly or independently. In the first case (1 step) the CAb-MBs were incubated for 30 min in the solution containing the target antigen supplemented with HRP-DAb, while in the second protocol (2 steps) two successive and independent 30-min incubation steps were performed in antigen and HRP-DAb solutions, respectively. Fig. 1c shows that while the B response did not vary significantly, a remarkably smaller S response was obtained when the 1-step protocol was used. These results can be justified by the poorer recognition of the target antigen marked with the HRP-DAb by the CAb-MBs with respect to the recognition of the free antigen. Accordingly, the two-step protocol was selected to perform the immunoassay. Thereafter, optimization of the incubation time of the CAb-MBs with the target antigen gave rise to the choice of 45 min (Fig. 1d).

Finally, the effect of the concentration (Fig. 1e) and the incubation time (Fig. 1f) with the HRP-DAb solution for the recognition and enzymatic labeling of the captured antigen on the MBs were evaluated. The selected values were 0.5 µg mL^{-1} and 15 min, respectively. Regarding the concentration of the detector antibody (Fig. 1e), the B responses increased progressively with the concentration. However, the S responses increased up to 1.0 µg mL^{-1} and levelled off for larger concentrations. Therefore, the S/B ratio increased with the HRP-DAb concentration up to 0.5 µg mL^{-1} and decreased slightly for higher concentrations. Fig. 1f shows as the dependence of the S and B responses with the incubation time in the HRP-DAb solution exhibited a similar trend. Since the S response increased less than the B response for incubation times longer than 15 min, a better S/B ratio was observed for this incubation time.

According to these optimization studies and counting since the formation of CAb-MBs, the determination of CA19-9 involves only 2 incubation steps and can be completed in 60 min. It is important to remark that no discrimination between S and B signals was possible in the absence of CAb and HRP-DAb (bars 0 in Fig. 1a and e). This proved the reliability of the used immunoassay format as well as the efficiency of the blocking step employed after the immobilization of the CAb on the MBs to avoid undesired non-specific adsorption of the HRP-DAb when no CA19-9 is present.

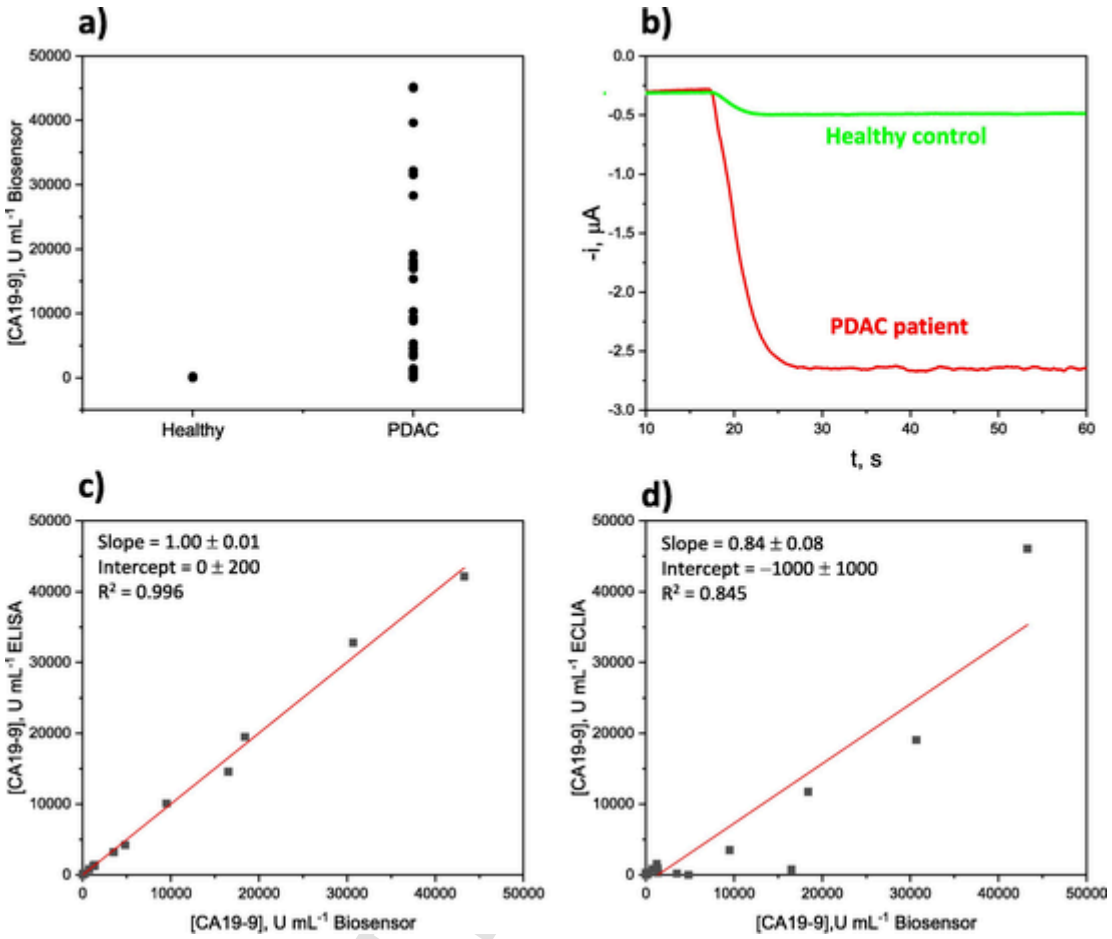

Fig. 5. a) concentration of ca19-9 determined with the developed immunoplatform in pooled serum samples (results obtained for all replicates are included). b) representative examples of the amperometric traces recorded with the bioplatforms for 50-fold diluted serum of a healthy individual and a pdac patient (samples healthy control 2 and pdac patient 13 in Table 2, respectively). Correlations between the results provided by the inmmunoplatform and c) the ELISA method using the same immunoreagents, and d) the ECLIA used at the Reference Laboratory.

3.2. Analytical and operational characteristics for the amperometric determination of CA19-9

Under the optimized experimental conditions, the relationship between the measured amperometric responses and the concentration of the target CA19-9 was established. The dose-dependent amperometric current values and the corresponding calibration plot are displayed in Fig. 2. A linear relationship between the amperometric readings and the target antigen concentration was found between the 5.0 to 500 U mL^{-1} CA19-9 concentration range (r^2 = 0.9946), with a slope and intercept values of (6.4 ± 0.5) × 10^{-3} µA mL U^{-1} and (12 ± 2) × 10^{-2} µA, respectively. The linear range is suitable to determine clinically relevant serum levels of CA19-9 in pancreatic cancer [53]. Moreover, limit of detection (LOD) and quantification (LOQ) values of 1.5 and 5.0 U mL^{-1}, respectively, were calculated according to the 3 × s_b/m and 10 × s_b/m criteria, respectively, where s_b is the standard deviation of 10 measurements of the blank solution in the absence of CA19-9, and m the slope of the linear calibration plot displayed in Fig. 2.

We compared the achieved analytical characteristic to those reported for other electrochemical biosensing strategies described in the last decade (summarized in Table 1). Although the achieved LOD with the immunoplatform is, in general, larger, the obtained sensitivity allows discrimination of healthy individuals from patients diagnosed with PDAC considering the established cut-off values for this biomarker in serum to discriminate between these two populations (130–338 U mL^{-1} [54–56]), making the immunoplatform fully compatible with its application in the clinic. In addition, the developed methodology uses disposable screen-printed electrodes, similarly to that reported by Ibánez-Redín *et al.* [38,39], which improves the simplicity of the method. In fact, unlike most of the reported strategies, our method does not require the preparation of nanomaterials, and involves shorter times for sample preparation as well as for the determination. These characteristics render the immunoplatform particularly attractive for implementation in POC application devices. It should also be noted that the developed immunoplatform for the determination of CA19-9 is the first one exploiting the advantages of using MBs in bioassay strategies in terms of sensitivity, rapid assay kinetics, and minimization of potential matrix effects [57–59]. Of note, the CA19-9 ELISA-based method used by reference laboratories allows the sensitive and selective determination of the target antigen. However, its cost and instrumentation characteristics restricts the use to centralized and resource-constrained environments, a limitation that can be overcome using the developed immunoplatform.

Another important feature of the developed immunoplatform is the high operational reproducibility concerning both the preparation of the magnetic bioconjugates and the amperometric transduction on SPCEs. Indeed, a relative standard deviation (RSD) value of 4.2 % was calculated using ten different bioplatforms prepared in the same way for the measurement of 250 U mL^{-1} CA19-9 standard.

Another relevant aspect to be highlighted is the storage stability of the CAb-MBs used as a basis for the immunoassay. The control graph shown in Fig. 3 displays the S/B ratios provided by the bioplatforms prepared each control day using the CAb-MBs stored after their prepa-

ration in filtered PBS at 4 °C. As it can be deduced, the S/B ratios remain within the control limits for three weeks.

3.3. Selectivity

Complex serum samples are characterized by containing a wide diversity and a variable level of biological entities of different omic levels. Considering this, the selectivity of the developed immunoplatform against potential interfering species that may be found in serum was evaluated.

The amperometric responses (and the corresponding S/B ratios) for 0 and 250 U mL^{-1} CA19-9 standards were measured in the absence and in the presence of different serum components at the expected concentrations in healthy individuals. As Fig. 4 shows, none of the tested components exhibited a significant effect on the sensitivity achieved in the determination of CA19-9.

3.4. Application to the analysis of serum samples from patients with pancreatic cancer

To assess the real biomedical application of the developed electrochemical immunoplatform, it was employed for the determination of CA19-9 in 22 serum samples (6 from healthy individuals and 16 from PDAC patients).

The possible matrix effect was evaluated by comparing the slope values of calibration plots prepared with buffered standard solutions of CA19-9 ($(6.4 \pm 0.5) \times 10^{-3}$ μA mL U^{-1}), and with a 50-fold diluted serum sample from a healthy individual supplemented with increasing concentrations of CA19-9 standards ($(5.5 \pm 0.1) \times 10^{-3}$ μA mL U^{-1}). The application of the Student's *t*-test ($t_{exp} = 1.69 < t_{tab} = 2.78$, $\alpha = 0.05$; $n = 5$) indicated that there were no significant differences between the slope values of both calibration curves. This allows discarding the existence of a significant matrix effect for the so diluted serum samples and performing the determination by simple interpolation of the amperometric readings obtained for the diluted serum samples into the calibration constructed with CA19-9 standards (Fig. 2 inset). The results obtained by triplicate for each sample are summarized in Table 2 and plotted in Fig. 5. In addition, Table 2 includes the results provided by the ELISA methodology using the same immunoreagents that in the developed immunoplatform, demonstrating the excellent concordance of the results using both techniques. In contrast, CA19-9 values obtained from the Barcelona Reference Laboratory using an electrochemiluminescence immunoassay (ECLIA) showed discrepant values in several samples (Table 2), likely due to differences in the immunoreagents or the analyzer used for this method (see below).

The results obtained with the immunoplatform demonstrate the possibility to discriminate healthy individuals from PDAC patients as well as show the wide CA19-9 concentration range found in the cohort of PDAC patients. According to the obtained results, while the CA19-9 concentration was not detectable in most of the healthy individuals (5 out of 6), i.e., below the estimated LOD of 1.5 U mL^{-1}, 13 of the 16 samples analyzed from PDAC patients had a much larger concentration than the normal value established in serum (< 37 U mL^{-1}) [53], with values varying between 190 and 43,000 U mL^{-1}. These results agree with the cut-off values set by Jans *et al.*, 130 U mL^{-1}, to predict malignancy [55], by Kilic *et al.,* 256.4 U mL^{-1}, to preoperatively determine the patients that have unresectable pancreatic cancer [54], and by Dong *et al.*, 338.45 U mL^{-1}, to predict poor prognosis in patients with resectable PDAC [56].

Regarding the comparison of the results provided by the immunoplatform with those using the ELISA and ECLIA, the correlation parameters shown in Fig. 5c and 5d confirm, as previously pointed out by other authors, that the results provided by methodologies using different immunoreagents should not be compared. The reason is that different antibodies can recognize different parts of the molecule, and antigen heterogeneity may account in part for inter-method differences [60]. This fact is clearly shown in the excellent correlation (with values of slope and intercept including 1 and 0, respectively) exhibited between the immunoplatform and ELISA as both methods used the same immunoreagents (Fig. 5c). However, a much poorer correlation was observed when the immunoplatform results were compared with those obtained by ECLIA (Fig. 5d), which measures CA19-9 using a different antibody, substrate and detector.

4. Conclusions

A new electrochemical immunoplatform for the determination of CA19-9 is reported. It involves the formation of sandwich immunoconjugates labeled with the HRP enzyme on the surface of MBs and amperometric transduction at SPCEs in the presence of HQ and H_2O_2.The immunoplatform exhibits analytical characteristics suitable to be clinically applicable, as it is able to discriminate between healthy individuals and subjects with PDAC and shows good selectivity and reproducibility. The immunoplatform showed good results for the determination of CA19-9 in a cohort of patients including healthy individuals and patients diagnosed with PDAC. It allowed the positive identification of these patients in only one hour and after a simple dilution of the sample. The developed immunoplatform is attractive compared to the reported electrochemical methodologies in terms of simplicity of fabrication and use. Moreover, it stands out in terms of cost and applicability at the point of care compared to the most currently used methodologies of ELISA and ECLIA with automatic analyzers. These are crucial aspects so that this minimally invasive determination of CA19-9 levels in serum may complement available technologies in the reliable and early diagnosis of PDAC. In addition, the test provided by the immunoplatform is within the reach of anyone regardless of their financial resources and due to its simplicity, low energy consumption and potential for miniaturization of the used instrumentation. Moreover, it may be available in different environments other than hospitals, as outpatient clinics or even as a home-based test run by the test subject.

5. Consent for publication

All authors consent to the publication of the manuscript in Journal of Electroanalytical Chemistry, should the article be accepted by the Editor-in-chief upon completion of the refereeing process.

CRediT authorship contribution statement

Víctor Pérez-Ginés : Methodology, Investigation, Writing – review & editing, Writing – original draft. **Rebeca M. Torrente-Rodríguez :** Supervision, Writing – review & editing, Writing – original draft. **María Pedrero :** Supervision, Writing – review & editing, Writing – original draft. **Neus Martínez-Bosch :** Conceptualization, Resources, Writing – review & editing, Writing – original draft. **Pablo García de Frutos :** Conceptualization, Resources, Writing – review & editing, Writing – original draft. **Pilar Navarro :** Conceptualization, Resources, Writing – review & editing, Writing – original draft. **José M. Pingarrón :** Resources, Writing – review & editing, Writing – original draft. **Susana Campuzano :** Conceptualization, Supervision, Resources, Writing – review & editing, Writing – original draft, Funding acquisition.

Declaration of Competing Interest

The authors declare that they have no known competing financial interests or personal relationships that could have appeared to influence the work reported in this paper.

Data availability

Data will be made available on request.

Acknowledgements

The financial support of PID2019-103899RB-I00 and the TRANSNANOAVANSENS-CM Program from the Comunidad de Madrid (Grant S2018/NMT-4349) to S.C. and from the Spanish Ministry of Science and Innovation (MICINN)/ Instituto de Salud Carlos III (ISCIII)-European Regional Development Fund (ERDF) (PI20/00625) to P.N. are gratefully acknowledged. V.P.G. acknowledges a predoctoral contract from Universidad Complutense de Madrid. We would also like to thank Dr. L. Visa (Oncology Department, Hospital del Mar), Dr. L.E. Barranco (Digestive Department, Hospital del Mar) and D. Zafra Puerta (Nursing Department, Hospital del Mar) for their valuable help with sample collection, as well as patients and their families who were enrolled in the project.

References

[1] M. Orth, P. Metzger, S. Gerum, J. Mayerle, G. Schneider, C. Belka, M. Schnurr, K. Lauber, Pancreatic ductal adenocarcinoma: biological hallmarks, current status, and future perspectives of combined modality treatment approaches, Radiat. Oncol. 14 (2019) 141, https://doi.org/10.1186/s13014-019-1345-6.

[2] M. Hidalgo, Pancreatic cancer, N. Engl. J. Med. 362 (17) (2010) 1605–1617.

[3] W. Petrushnko, J.S. Gundara, P.R. De Reuver, G. O'Grady, J.S. Samra, A. Mittal, Systematic review of peri-operative prognostic biomarkers in pancreatic ductal adenocarcinoma, HPB 18 (2016) 652–663, https://doi.org/10.1016/j.hpb.2016.05.004.

[4] E. Ermiah, M. Eddfair, O. Abdulrahman, M. Elfagieh, A. Jebriel, M. Al-Sharif, M. Assidi, A. Buhmeida, Prognostic value of serum CEA and CA19-9 levels in pancreatic ductal adenocarcinoma, Mol. Clin. Oncol. 17 (2022) 126, https://doi.org/10.3892/mco.2022.2559.

[5] R.L. Siegel, K.D. Miller, N.S. Wagle, A. Jemal, Cancer statistics, CA, Cancer J. Clin. 73 (2023) 17–48, https://doi.org/10.3322/caac.21763.

[6] D.K. Owens, K.W. Davidson, A.H. Krist, M.J. Barry, M. Cabana, A.B. Caughey, S.J. Curry, C.A. Doubeni, J.W. Epling, M. Kubik, C.S. Landefeld, C.M. Mangione, L. Pbert, M. Silverstein, M.A. Simon, C.-W. Tseng, J.B. Wong, Screening for pancreatic cancer: US preventive services task force reaffirmation recommendation statement, JAMA 322 (5) (2019) 438.

[7] S. Modi, D. Kir, A.K. Saluja, Old dog, new tricks: use of CA 19–9 for early diagnosis of pancreatic cancer, Gastroenterology 160 (2021) 1019–1021, https://doi.org/10.1053/j.gastro.2021.01.001.

[8] B. Turanli, E. Yildirim, G. Gulfidan, K.Y. Arga, R. Sinha, Current state of "omics" biomarkers in pancreatic cancer, J. Pers. Med. 11 (2021) 127, https://doi.org/10.3390/jpm11020127.

[9] B. George, M. Kent, A. Surinach, N. Lamarre, P. Cockrum, The association of real-world CA19-9 level monitoring patterns and clinical outcomes among patients with metastatic pancreatic ductal adenocarcinoma, Front. Oncol. 11 (2021) 754687, https://doi.org/10.3389/fonc.2021.754687.

[10] L.E. Kane, G.S. Mellotte, K.C. Conlon, B.M. Ryan, S.G. Maher, Multi-omic biomarkers as potential tools for the characterisation of pancreatic cystic lesions and cancer: innovative patient data integration, Cancers 13 (2021) 769, https://doi.org/10.3390/cancers13040769.

[11] B.J.C. Yong, M.W. Diyana, Low carbohydrate antigen 19–9 (CA19-9) levels in a patient highly suspected of having caput pancreas tumor, Cureus 14 (2022) e24357.

[12] A. Coppola, V. La Vaccara, T. Farolfi, M. Fiore, R. Cammarata, S. Ramella, R. Coppola, D. Caputo, Role of CA 19.9 in the management of resectable pancreatic cancer: State of the art and future perspectives, Biomedicines 10 (9) (2022 2091.) 2091.

[13] E. Buscail, C. Maulat, F. Muscari, L. Chiche, P. Cordelier, S. Dabernat, C. Alix-Parabières, L. Buscali, Liquid biopsy approach for pancreatic ductal adenocarcinoma, Cancers 11 (2019) 852, https://doi.org/10.3390/cancers11060852.

[14] H. Wu, S. Ou, H. Zhang, R. Huang, S. Yu, M. Zhao, S. Tai, Advances in biomarkers and techniques for pancreatic cancer diagnosis, Cancer Cell Int. 22 (2022) 220, https://doi.org/10.1186/s12935-022-02640-9.

[15] L.C. Chu, M.G. Goggins, E.K. Fishman, Diagnosis and detection of pancreatic cancer, Cancer J. 23 (2017) 333–342, https://doi.org/10.1097/PPO.0000000000000290.

[16] N. Kamyabi, V. Bernard, A. Maitra, Liquid biopsies in pancreatic cancer, Expert Rev. Anticancer. Ther. 19 (10) (2019) 869–878, https://doi.org/10.1080/14737140.2019.1670063.

[17] M.E. Herrero-Zabaleta, R. Gautier, P. Burtin, N. Daher, J. Bara, Monoclonal antibody against sialylated Lewis (a) antigen, Bull Cancer. 74 (4) (1987) 387–396.

[18] T. Yue, K. Partyka, K.A. Maupin, M. Hurley, P. Andrews, K. Kaul, A.J. Moser, H. Zeh, R.E. Brand, B.B. Haab, Identification of blood-protein carriers of the CA 19–9 antigen and characterization of prevalence in pancreatic diseases, Proteomics 11 (2011) 3665–3674, https://doi.org/10.1002/pmic.201000827.

[19] H.S. Lee, C.Y. Jang, S.A. Kim, S.B. Park, D.E. Jung, B.O. Kim, H.Y. Kim, M.J. Chung, J.Y. Park, S. Bang, S.W. Park, S.Y. Song, Combined use of CEMIP and CA 19–9 enhances diagnostic accuracy for pancreatic cancer, Sci. Rep. 8 (2018) 3383, https://doi.org/10.1038/s41598-018-21823-x.

[20] C.L. Diaz, P. Cinar, J. Hwang, A.H. Ko, M.A. Tempero, CA 19–9 response: a surrogate to predict survival in patients with metastatic pancreatic adenocarcinoma, Am. J. Clin. Oncol. 42 (2019) 898–902, https://doi.org/10.1097/COC.0000000000000620.

[21] A. Chan, I. Prassas, A. Dimitromanolakis, R.E. Brand, S. Serra, E.P. Diamandis, I.M. Blasutig, Validation of biomarkers that complement CA19.9 in detecting early pancreatic cancer, Clin. Cancer Res. 20 (22) (2014) 5787–5795.

[22] L.E. Kane, G.S. Mellotte, E. Mylod, R.M. O'Brien, F. O'Connell, C.E. Buckley, J. Arlow, K. Nguyen, D. Mockler, A.D. Meade, B.M. Ryan, S.G. Maher, Diagnostic accuracy of blood-based biomarkers for pancreatic cancer: a systematic review and meta-analysis, Cancer Res. Commun. 2 (10) (2022) 1229–1243.

[23] L.N.C. Boyd, M. Ali, M.M.G. Leeflang, G. Treglia, R. de Vries, T.Y.S. Le Large, M.G. Besselink, E. Giovannetti, H.W.M. van Laarhoven, G. Kazemier, Diagnostic accuracy and added value of blood-based protein biomarkers for pancreatic cancer: a meta-analysis of aggregate and individual participant data, EClinicalMedicine 55 (2023) 101747, https://doi.org/10.1016/j.eclinm.2022.101747.

[24] S. Salleh, A. Thyagarajan, R.P. Sahu, Exploiting the relevance of CA 19–9 in pancreatic cancer, J. Cancer Metastasis Treat. 6 (2020) 31, https://doi.org/10.20517/2394-4722.2020.70.

[25] K.E. Poruk, D.Z. Gay, K. Brown, J.D. Mulvihill, K.M. Boucher, C.L. Scaife, M.A. Firpo, S.J. Mulvihill, The clinical utility of CA19-9 in pancreatic adenocarcinoma: diagnostic and prognostic updates, Curr. Mol. Med. 13 (2013) 340–351, https://doi.org/10.2174/1566524011313030003.

[26] J.L. Humphris, D.K. Chang, A.L. Johns, C.J. Scarlett, M. Pajic, M.D. Jones, E.K. Colvin, A. Nagrial, V.T. Chin, L.A. Chantrill, J.S. Samra, A.J. Gill, J.G. Kench, N.D. Merrett, A. Das, E.A. Musgrove, R.L. Sutherland, A.V. Biankin, The prognostic and predictive value of serum CA19.9 in pancreatic cancer, Ann. Oncol. 23 (2012) 1713–1722, https://doi.org/10.1093/annonc/mdr561.

[27] G. Luo, M. Guo, K. Jin, Z. Liu, C. Liu, H.e. Cheng, Y.u. Lu, J. Long, L. Liu, J. Xu, Q. Ni, X. Yu, Optimize CA19-9 in detecting pancreatic cancer by lewis and secretor genotyping, Pancreatology 16 (6) (2016) 1057–1062.

[28] G. Luo, K. Jin, M. Guo, H. Cheng, Z. Liu, Z. Xiao, Y. Lu, J. Long, L. Liu, J. Xu, C. Liu, Y. Gao, Q. Ni, X. Yu, Patients with normal-range CA19-9 levels represent a distinct subgroup of pancreatic cancer patients, Oncol. Lett. 13 (2017) 881–886, https://doi.org/10.3892/ol.2016.5501.

[29] F.X. Hu, S.H. Chen, R. Yua, Application of magnetic core–shell microspheres on reagentless immunosensor based on direct electrochemistry of glucose oxidase for detection of carbohydrate antigen 19–9, Sens. Actuators, B 176 (2013) 713–722, https://doi.org/10.1016/j.snb.2012.08.072.

[30] G. Wang, Y. Qing, J. Shan, F. Jin, R. Yuan, D. Wang, Cation-exchange antibody labeling for simultaneous electrochemical detection of tumor markers CA15-3 and CA19-9, Microchim. Acta 180 (2013) 651–657, https://doi.org/10.1007/s00604-013-0973-z.

[31] Q. Zhang, X. Chen, Y. Tang, L. Ge, B. Guo, C. Yao, Amperometric carbohydrate antigen 19–9 immunosensor based on three dimensional ordered macroporous magnetic Au film coupling direct electrochemistry of horseradish peroxidase, Anal. Chim. Acta 815 (2014) 42–50, https://doi.org/10.1016/j.aca.2014.01.033.

[32] Z. Jiang, C. Zhao, L. Lin, S. Weng, Q. Liu, X. Lin, A label-free electrochemical immunosensor based on poly(thionine)–SDS nanocomposites for CA19-9 detection, Anal. Methods 7 (2015) 4508–4513, https://doi.org/10.1039/C5AY00576K.

[33] Y. Xie, X. Zhi, H. Su, K. Wang, Z. Yan, N. He, J. Zhang, D. Chen, D. Cui, A novel electrochemical microfluidic chip combined with multiple biomarkers for early diagnosis of gastric cancer, Nanoscale Res. Lett. 10 (2015) 477, https://doi.org/10.1186/s11671-015-1153-3.

[34] Z. Huang, Z. Jiang, C. Zhao, W. Han, L. Lin, A. Liu, S. Weng, X. Lin, Simple and effective label-free electrochemical immunoassay for carbohydrate antigen 19–9 based on polythionine-Au composites as enhanced sensing signals for detecting different clinical samples, Int. J. Nanomed. 12 (2017) 3049–3058, https://doi.org/10.2147/IJN.S131805.

[35] X. Weng, Y. Liu, Y. Xue, A.-J. Wang, L. Wu, J.-J. Feng, L-Proline bio-inspired synthesis of AuPt nanocalliandras as sensing platform for label-free electrochemical immunoassay of carbohydrate antigen 19–9, Sens. Actuat. B Chem. 250 (2017) 61–68, https://doi.org/10.1016/j.snb.2017.04.156.

[36] A. Thapa, A.C. Soares, J.C. Soares, I.T. Awan, D. Volpati, M.E. Melendez, J.H.T.G. Fregnani, A.L. Carvalho, O.N. Oliveira, Carbon nanotube matrix for highly sensitive biosensors to detect pancreatic cancer biomarker CA19-9, ACS Appl. Mater. Interfaces 9 (31) (2017) 25878–25886.

[37] A.C. Soares, J.C. Soares, F.M. Shimizu, V.d.C. Rodrigues, I.T. Awan, M.E. Melendez, M.H.O. Piazzetta, A.L. Gobbi, R.M. Reis, J.H.T.G. Fregnani, A.L. Carvalho, O.N. Oliveira, A simple architecture with self-assembled monolayers to build immunosensors for detecting the pancreatic cancer biomarker CA19-9, Analyst 143 (14) (2018) 3302–3308.

[38] G. Ibáñez-Redín, R.H.M. Furuta, D. Wilson, F.M. Shimizu, E.M. Materon, L.M.R.B. Arantes, M.E. Melendez, A.L. Carvalho, R.M. Reis, M.N. Chaur, D. Gonçalves, O.N. Oliveira, Screen-printed interdigitated electrodes modified with nanostructured carbon nano-onion films for detecting the cancer biomarker CA19-9, Mater. Sci. Eng. C 99 (2019) 1502–1508, https://doi.org/10.1016/j.msec.2019.02.065.

[39] G. Ibáñez-Redín, E.M. Materon, R.H.M. Furuta, D. Wilson, G.F. do Nascimento, M.E. Melendez, A.L. Carvalho, R.M. Reis, O.N. Oliveira, D. Gonçalves, Screen-

printed electrodes modified with carbon black and polyelectrolyte films for determination of cancer marker carbohydrate antigen 19–9, Microchim. Acta 187 (7) (2020), https://doi.org/10.1007/s00604-020-04404-6.
[40] T. Kalyani, A. Sangili, A. Nanda, S. Prakash, A. Kaushik, S.K. Jana, Bio-nanocomposite based highly sensitive and label-free electrochemical immunosensor for endometriosis diagnostics application, Bioelectrochemistry 139 (2021) 107740, https://doi.org/10.1016/j.bioelechem.2021.107740.
[41] Y. An, L. Song, X. Chen, C. Ni, K. Mao, L. Zhu, Y. Gu, Y. Miao, B. Song, H. m, 3D biomimetic hydrangea-like BiOCl and PtNi nanocube-based electrochemical immunosensor for quantitative detection of CA19–9, J. Electrochem. Soc. 169 (2022) 056520, https://doi.org/10.1149/1945-7111/ac700c.
[42] R. Qiu, J. Dai, L. Meng, H. Gao, M. Wu, F. Qi, J. Feng, H. Pan, A novel electrochemical immunosensor based on COF-LZU1 as precursor to form heteroatom-doped carbon nanosphere for CA19-9 detection, Appl. Biochem. Biotechnol. 194 (2022) 3044–3065, https://doi.org/10.1007/s12010-022-03861-4.
[43] Q. Wang, F. Chen, L. Qiu, Y. Mu, S. Sun, X. Yuan, P. Shang, B. Ji, Detection of esophageal cancer marker CA19-9 based on MXene electrochemical immunosensor, Int. J. Electrochem. Sci. 17 (2022). 220712. https://doi.org/10.20964/2022.07.07.
[44] Z. Wei, X. Cai, W. Cui, J. Zhang, Electrochemical immunoassay for tumor marker CA19-9 detection based on self-assembled monolayer, Molecules 27 (2022) 4578, https://doi.org/10.3390/molecules27144578.
[45] A. Ben Aissa, J.J. Jara, R.M. Sebastián, A. Vallribera, S. Campoy, M.I. Pividori, Comparing nucleic acid lateral flow and electrochemical genosensing for the simultaneous detection of foodborne pathogens, Biosens. Bioelectron. 88 (2017) 265–272, https://doi.org/10.1016/j.bios.2016.08.046.
[46] M. Bartosik, L. Jirakova, M. Anton, B. Vojtesek, R. Hrstka, Genomagnetic LAMP-based electrochemical test for determination of high-risk HPV16 and HPV18 in clinical samples, Anal. Chim. Acta 1042 (2018) 37–43, https://doi.org/10.1016/j.aca.2018.08.020.
[47] C. Munoz-San Martin, M. Gamella, M. Pedrero, A. Montero-Calle, R. Barderas, S. Campuzano, J.M. Pingarrón, Magnetic beads-based electrochemical immunosensing of HIF-1α, a biomarker of tumoral hypoxia, Sens. Actuat. B 307 (2020) 127623, https://doi.org/10.1016/j.snb.2019.127623.
[48] M. Eguílaz, M. Moreno-Guzmán, S. Campuzano, A. González-Cortés, P. Yáñez-Sedeño, J.M. Pingarrón, An electrochemical immunosensor for testosterone using functionalized magnetic beads and screen-printed carbon electrodes, Biosens. Bioelectron. 26 (2010) 517–522, https://doi.org/10.1016/j.bios.2010.07.060.
[49] F. Conzuelo, M. Gamella, S. Campuzano, D.G. Pinacho, A.J. Reviejo, M.P. Marco, J.M. Pingarrón, Disposable and integrated amperometric immunosensor for direct determination of sulfonamide antibiotics in milk, Biosens. Bioelectron. 36 (2012) 81–88, https://doi.org/10.1016/j.bios.2012.03.044.
[50] B. Esteban-Fernández de Ávila, V. Escamilla-Gómez, S. Campuzano, M. Pedrero, J.P. Salvador, P.M. Marco, J.M. Pingarrón, Ultrasensitive amperometric magnetoimmunosensor for human C-reactive protein quantification in serum, Sens. Actuat. B Chem. 188 (2013) 212–220, https://doi.org/10.1016/j.snb.2013.07.026.
[51] R.M. Torrente-Rodríguez, V.R. Valdepeñas-Montiel, S. Campuzano, M. Pedrero, M. Farchado, E. Vargas, F.J. Manuel de Villena, M. Garranzo-Asensio, R. Barderas, J.M. Pingarrón, Electrochemical sensor for rapid determination of fibroblast growth factor receptor 4 in raw cancer cell lysates, PLoS ONE 12 (2017) e0175056.
[52] P. Bhadra, M.S. Shajahan, E. Bhattacharya, A. Chadha, Studies on varying n-alkanethiol chain lengths on a gold coated surface and their effect on antibody–antigen binding efficiency, RSC Adv. 5 (2015) 80480–80487, https://doi.org/10.1039/C5RA11725A.
[53] U.K. Ballehaninna, R.S. Chamberlain, Serum CA 19–9 as a biomarker for pancreatic cancer–A comprehensive review, Indian J. Surg. Oncol. 2 (2) (2011) 88–100, https://doi.org/10.1007/s13193-011-0042-1.
[54] M. Kiliç, E. Göçmen, M. Tez, T. Ertan, M. Keskek, M. Koç, Value of preoperative serum CA 19–9 levels in predicting resectability for pancreatic cancer, Can J. Surg. 49 (4) (2006) 241–244.
[55] J. Jans, M.J. Talma, M. Almonacid, J. Cruz, M. Cáceres, C. Rosenfeld, G. Jara, Rendimiento diagnóstico del marcador tumoral CA 19–9 en la diferenciación entre patología bilio-pancreática benigna y maligna, Rev. Chil. Cir. 65 (4) (2013) 307–314, https://doi.org/10.4067/S0718-40262013000400004.
[56] Q. Dong, X.-H. Yang, Y. Zhang, W. Jing, L.-Q. Zheng, Y.-P. Liu, X.-J. Qu, Elevated serum CA19-9 level is a promising predictor for poor prognosis in patients with resectable pancreatic ductal adenocarcinoma: a pilot study, World J. Surg. Oncol. 12 (2014) 171. http://www.wjso.com/content/12/1/171.
[57] M.E. Cortina, L.J. Melli, M. Roberti, M. Mass, G. Longinotti, S. Tropea, P. Lloret, D.A. Rey Serantes, F. Salomón, M. Lloret, A.J. Caillava, S. Restuccia, J. Altcheh, C.A. Buscaglia, L. Malatto, J.E. Ugalde, L. Fraigi, C. Moina, G. Ybarra, A.E. Ciocchini, D.J. Comerci, Electrochemical magnetic microbeads-based biosensor for point-of-care serodiagnosis of infectious diseases, Biosens. Bioelectron. 80 (2016) 24–33, https://doi.org/10.1016/j.bios.2016.01.021.
[58] J. Kudr, B. Klejdus, V. Adam, O. Zitka, Magnetic solids in electrochemical analysis, TrAC Trends, Anal Chem. 98 (2018) 104–113, https://doi.org/10.1016/j.trac.2017.10.023.
[59] M. Pastucha, Z. Farka, K. Lacina, Z. Mikušová, P. Skládal, Magnetic nanoparticles for smart electrochemical immunoassays: a review on recent developments, Microchim. Acta. 186 (2019) 312, https://doi.org/10.1007/s00604-019-3410-0.
[60] N. Serdarevic, The comparison between different immunoassays for serum carbohydrate antigen (CA 19–9) concentration measurement, Acta Inform. Med. 26 (4) (2018) 235–239, https://doi.org/10.5455/aim.2018.26.235–239.